Int. J. Morphol.,
43(6):1843-1856, 2025.

Renal Protective Effect of *Ginkgo biloba* Extract Against Amiodarone-induced Toxicity, Oxidative Stress and Injury

Efecto Protector Renal del Extracto de *Ginkgo biloba* Frente a la Toxicidad Inducida por Amiodarona, el Estrés Oxidativo y las Lesiones

Samy A. Dawood[1]; Refaat A. Eid[2]; Alsaleem Mohammed Abadi[3]; Ayed A. Shati[1]; Salim Jamil[2]; Attalla F. El-kott[4,5]; Gamal Mohamed[6]; Mubarak Al-Shraim[2]; Yhaya Abu Hamad[7]; Ali GadKarim A. Salih[8]; Tarig Gasim Mohamed Alarabi[8]; Safa Mousa Al-Haider[1]; Esmael M. Alyami[9] & Mohamed Samir A. Zaki[8]

DAWOOD, S. A.; EID, R. A.; ABADI, A. M.; SHATI, A. A.; JAMIL, S.; EL-KOTT, A. F.; MOHAMED, G.; AL-SHRAIM, M.; HAMAD, Y. A.; SALIH, A. G. A.; ALARABI, T. G. M.; AL-HAIDER, S. M.; ALYAMI , E. M. & ZAKI, M. S. A. Renal protective Ginkgo biloba extract against amiodarone-induced toxicity, oxidative stress and injury. *Int. J. Morphol., 43(6)*:1843-1856, 2025.

SUMMARY: Amiodarone (AMD) is categorized as an antiarrhythmic. Serious side effects of the treatment included a significant reduction in renal function. Extract from Ginkgo biloba leaves (GBL) has been shown to be an effective free radical scavenger and antioxidant. The purpose of this study was to evaluate the effect of GBL extract on nephrotoxicity brought on by AMD. Forty male rats were divided into four groups. Control in Group I. Group II got GBL extract. On the 21st day, AMD group received an intraperitoneal (i.p.) injection of AMD. In GBL plus AMD group, rats received GBL for 21 days before receiving AMD. After four weeks, the rats were sacrificed, and their kidneys were removed for histological, ultrastructural, N-acetyl-beta-D glycosaminidase (NAG) levels, renal function markers like serum urea, creatinine, protein excretion rate, inflammatory cytokines and oxidative stress markers were determined. AMD-induced kidney damage in rats may be brought on by oxidative stress producing significant renal cytotoxicity, as evidenced by biochemical, histopathological, and electron microscopy investigations. After administering GBL extract to AMD group, every parameter that was looked at through this study was significantly improved. According to the current study's findings, GBL extract reduced AMD-induced nephrotoxicity by acting as an antioxidant.

KEY WORDS: Amiodarone; Nephrotoxicity; *Ginkgo biloba*; Histopathology; Renal function markers; NAG.

INTRODUCTION

Because of its ease, efficacy, and minimal inotropic effects, amiodarone (AMD), was an appropriate antiarrhythmic medicine utilized for cardiac dysfunctions and heart arrhythmias treatment (Ono *et al*., 2022; Deng *et al*., 2022). Despite its therapeutic action, however, may be toxic to different organ systems (Ebeid *et al*., 2023). Multiple organs and tissues experienced toxicities because of the long-term use of AMD at an accumulative dosage (Istratoaie *et al*., 2021). A reasonably frequent and treatable cause of acute kidney injury, drug-induced nephrotoxicity, can be identified and treated early. Drug-drug interactions' pharmacokinetics or pharmacodynamics might result in additive or synergistic toxicity. Additional nephrotoxicities, which are frequently difficult to foresee or detect, can result from the introduction of new drugs or from the usage of drugs outside of the recommended dosage in a critical care situation (Zhu *et al*.,

[1] Department of Child Health, College of Medicine, King Khalid University, Abha, Saudi Arabia. (samyshorbagy8@hotmail.com, ashati@kku.edu.sa, S22alhaider@hotmail.com).
[2] Department of Pathology, College of Medicine, King Khalid University, Abha, Saudi Arabia. (raeid@kku.edu.sa), (abdalmatian@kku.edu.sa), (malshraim@kku.edu.sa).
[3] Department of Family and Community Medicine, College of Medicine, King Khalid University, Abha, Saudi Arabia (Mabade@kku.edu.sa).
[4] Department of Biology, College of Science, King Khalid University, Abha 61421, Saudi Arabia (elkottaf@yahoo.com).
[5] Department of Zoology, College of Science, Damanhour University, Damanhour 22511, Egypt (elkottaf@yahoo.com).
[6] Department of Human Anatomy, Faculty of Medicine, Jazan University, Jazan, Saudi Arabia (gmahmed@jazanu.edu.sa).
[7] College of Medicine, King Khalid University, Abha, Saudi Arabia (yabohmad@kku.edu.sa).
[8] Department of Anatomy, College of Medicine, King Khalid University, Abha, Saudi Arabia (mszaki@kku.edu.sa), (aligadn@yahoo.com), (tahmed@kku.edu.sa).
[9] Department of Biology, College of Science, King Khalid University, PO Box 960, Asir, Abha, 61421, Saudi Arabia, (ealshahi@kku.edu.sa).
FUNDED. The authors received funding from the Deanship of Scientific Research at King Khalid University for this work (Grant No. RGP2/112/46).

Received: 2025-03-17 Accepted: 2025-08-26

2023). Additionally, there are an exponentially growing number of novel pharmaceuticals being developed, including chemotherapeutics and biological agents that may have nephrotoxic effects (Gray *et al*., 2022).

The formation and accumulation of free radicals and reactive oxygen species (ROS) increased by AMD therapy led to damage to the DNA and cellular structure, which led to diseases in stress-prone organs like the kidney, liver, adrenal, and testis(Mihoubi *et al*., 2022; Liu *et al*., 2022). Antioxidants that mitigate these cellular damages may reduce oxidative stress and phospholipidosis in AMD-induced toxicity (Tummino *et al*., 2021).

The kidney is essential to human physiology. Its problems are thought to be a key contributor to disability and, in the worst cases, to death (Das *et al*., 2017). A major contributing factor to acute and chronic renal failure illnesses is drug-induced renal impairment (Worth *et al*., 2022).

Many disorders are treated using natural supplements, either to increase the effectiveness of the medication or to reduce its hazardous side effects (Shalen *et al*., 2021). *Ginkgo biloba* leaves (GBL) extract has been used extensively in traditional Chinese medicine for decades as one of the most popular herbal supplements (Vamos *et al*., 2022). G. biloba polysaccharides, according to several researchers, exhibit a variety of biological effects, including those that are antioxidative, anti-inflammatory, immunomodulatory, and anti-tumor (Razna *et al*., 2020).

One of the most popular phytotherapeutic medications in the world, GBL is a traditional Chinese herbal remedy with a long history of clinical use (Biernacka *et al*., 2023). It contains antioxidant and anti-inflammatory properties, according to recent pharmacological investigations (Razna *et al*., 2020), and anti-platelet aggregation properties (Cui *et al*., 2019). The primary ingredients that perform its biological actions are terpene Tri lactones and flavanol glycosides (Wang *et al*., 2023) and offer defense against oxidative cell injury (Wang *et al*., 2021). GBL extract is a nutraceutical herbal ingredient (Tousson *et al*., 2019). It has large concentrations of glycosides, flavonoids, terpenoids, diterpenes, sesquiterpenes, flavanols, and polyphenols, which have antioxidant properties, scavenge ROS, and protect against oxidative cell injury (Behl *et al*., 2022; Noor *et al*., 2022) .

GBL has been shown to have nephroprotective properties against methotrexate (Marin *et al*., 2022), gentamicin, and cisplatin- triggered kidney impairment and nephrotoxicity (Fang *et al*., 2021; Wei *et al*., 2022). In addition to increasing blood flow, the GBL extract also reduced platelet aggregation and pro-inflammatory activities (Li *et al*., 2022; Tao *et al*., 2022).

Creatinine and urea are undesirable byproducts of protein metabolism that must be expelled by the kidney; thus, a significant rise in these parameters, as seen in this study, shows functional kidney impairment (Nayok *et al*., 2022). Urea level can be raised by a variety of different factors, including dehydration, antidiuretic medication, and food, whereas creatinine is more relevant to the kidney since renal injury is the only important factor that raises the serum creatinine level (Miano *et al*., 2022).

A sensitive biomarker of renal parenchymal sickness is urinary N-acetyl-beta-D glycosaminidase (NAG) (Mishra *et al*., 2012; Popa *et al*., 2022). A lysosomal enzyme called NAG, which primarily comes from proximal tubular cells, passes into urine. This enzyme is characterized as being more sensitive to renal tubular damage and more selective. Due to NAG's stability in urine and its minimal individual variation, which allows excellent reproducibility when using colorimetric and spectrophotometric methods, a spot urine sample may usually be used for the assay (Çuhadar & Semerci, 2016; Wei *et al*., 2022).

To determine if GBL protects adult male rats from developing kidney damage caused by AMD, the current investigation was conducted which is accomplished through the histological, ultrastructural, NAG levels, renal function markers like serum urea, creatinine, protein excretion rate, inflammatory cytokines, and oxidative stress markers.

MATERIAL AND METHOD

Material. AMD were purchased from nearby pharmacies in Jeddah, Saudi Arabia. All chemicals and kits with high analytical grade were purchased from Biosystems (Barcelona, Spain). The urine NAG level was assessed by a colorimetric method utilizing a Nittobo Medial Co., Ltd. (Tokyo, Japan) reagent and a JCA-BM 6010/c automated chemistry analyzer (JEOL Ltd., Tokyo, Japan). Malondialdehyde (MDA) (cat. MBS268427), glutathione peroxidase (GPX) (cat MBS046356) and catalase (CAT) (cat MBS9712526) were analyzed using special ELISA kits for rats, My BioSource, CA, s).

Experimental rats and Diet. We acquired 40 mature male Wister rats from the King Khalid Medical College Animal House, each weighing 170±10 grams. They were housed in the identical settings as laboratory rats and provided a diet similar to that of AIN-93 (Reeves *et al*., 1993). They were maintained in accordance with the policies of the King Khalid Research Center.

Induction of nephrotoxicity. Rats were given a single 50 mg/kg injection of AMD to generate nephrotoxicity (Morales *et al*., 2003).

Collecting GBL. The leaves of GBL were collected from Sulaymaniyah north of Baghdad, Iraq, in September 2021, then washed with deionized water, dried in shade for several days at room temperature, and ground to powder.

Preparation of GBL extract. GBL was crushed to a fine powder (500 g) and preserved in one liter of ethanol (80 %) at room temperature. They were then combined for 48 hours with a magnetic stirrer at a speed of 100 rpm. Using a rotary evaporator, the extract was concentrated under vacuum at 40 °C. The condensed residue was then freeze-dried, and it was stored at 4 °C in non-permeable glass containers until it was needed (Shahidi *et al*., 2021).

Experimental design. For this investigation, King Khalid University College of Medicine contributed twenty-four mature male Wistar albino rats. Each rat weighed 200 ± 50 g and was given free access to tap water and a pure diet, AIN-93M (Research Diets, NJ, USA). Four groups of rats were created, with each group receiving adequate care to reduce pain or suffering. In addition, the welfare of experimental rats was carefully monitored, and appropriate measures were taken to ensure maximum welfare. The research ethics committee at King Khalid University approved the experimental approach, which was associated with the implementation to be used and managed by laboratory animals from the National Institutes of Health (NIH Publication No. 85-23, updated 1985). Following acclimation to the laboratory environment for two weeks, the rats were split into four groups of six rats each. The groups formed can be described as follows: There were four groups of rats, each with ten rats. Group I (Control): supplied with distilled water and under the same laboratory conditions. Group II (Sham operated): got 100 mg/kg b.wt. of GBL extract (Newman *et al*., 1998). Group III (AMD): were i.p. administered on day 21 with a single dose of AMD at a dose of 50 mg/kg after receiving distilled water for 3 weeks (Morales *et al*., 2003). Group IV (GBL + AMD): obtained i.p. injections of AMD on day 21 after receiving 100 mg/kg b.wt. of GBL extract for 21 days.

After 24-h urine sampling, ketamine (75 mg/kg intraperitoneally) and xylazine (13 mg/kg intraperitoneally) were used to anesthetize the animals. Under anesthesia, renal blood samples were collected from the rats and kidney samples were obtained. Before being employed for biochemical analysis, the obtained serum samples were separated and kept at -80 °C.

Paraffin section preparation. After the eighth week of therapy, the animals underwent light diethyl ether anesthesia before being dissected to eliminate the kidney. A 24-hour fixation in 10 % neutral buffered formalin was performed after cutting the kidney into small sections, each measuring about three mm3. The samples were washed to remove excess fixative, dehydrated in ascending ethyl alcohol grades, then cleaned twice with xylene. After that, the specimens were impregnated with paraffin. According to (Mitsa *et al*., 2022), pieces of (4-5 μm) thick were cut with a microtome, stained with hematoxylin and eosin, and inspected under a light microscope for histological evaluation. Using an Olympus BX50 light microscope (Tokyo, Japan), histopathological analysis was performed. The King Khalid University, College of Medicine's Department of Pathology examined the samples.

Electron microscopy preparation. All animal groups' kidney specimens were dissected into small pieces, each measuring about one mm3, and then immediately fixed at 4 OC for 18–24 h in freshly 3 % glutaraldehyde–formaldehyde. After cleaning the samples in phosphate buffer (pH 7.4), postfix them for an hour at 4 °C in isotonic 1 % osmium tetroxide. Sections were prepared for electron microscopic analysis using the technique of. To discover the area of interest, semithin sections were stained with toluidine blue. Next, ultrathin sections were created using glass knives and an ultra-microtome. JEOL JEM-1011 transmission electron microscope used for examination after being stained with uranyl acetate and lead citrate (Lan *et al*., 2022).

Determination of renal functional markers. Creatinine and urea levels in the blood were measured using an auto-analyzer (Olympus AU-600, Tokyo, Japan) in accordance with commercial kit protocols. Protein excretion rate was determined by turbidimetric determination of total protein in 24-h urine samples (Santos *et al*., 2020).

Urinary N-acetyl-beta-D glycosaminidase (NAG). Rats were individually housed in metabolic cages which allowed for urine collection. Urine was collected for NAG an assessment level. Using spectrophotometry, urinary NAG was measured. NAG hydrolyzes 2-Methoxy-4-(2-nitrovinyl)-phenyl 2-acetamido-2-deoxy-b-D-glucopyranoside (MNP-Lc NAc) to produce 2-Methoxy-4-(2-nitrovinyl)-phenol. Using a Shimadzu UV- Visible spectrophotometer model 2550, a reddish color is created upon addition of an alkaline buffer (pH 9.5), which can be detected at 505 nm (Çuhadar & Semerci, 2016).

Measurement of oxidative stress biomarkers. The kidney levels of MDA, as the marker of lipid peroxidation, were assessed according to Thio barbituric acid (TBA) test (Ohkawa *et al*., 1979). The absorbance was spectrophotometrically determined at 532 nm.

The kidney activities of glutathione peroxidase (GPX) were established according to the method of Rotruck and colleagues (Rotruck *et al*., 1973). The absorbance was determined at 420 nm using an ELISA reader and GPX activity is shown as U/mg protein.

The assay of CAT activities in kidney was carried out based on the Sinha method (Sinha, 1972). For initiation of the reaction, a sample (20 µL of supernatant) was added in 2 ml of 30 mM hydrogen peroxide (H_2O_2) in a 50 mM potassium phosphate buffer with pH 7.0. Enzyme units were considered as mM of used H_2O_2 per min g or mL.

Statistical Analysis. Mean ± SD error (SE) was used to represent all values. Multiple group comparisons were conducted using a one-way ANOVA test, followed by LSD test for biochemical parameters and the Dunnett T3 test for real-time RT-PCR findings. The SPSS statistics program (version 20) was used for statistical analysis. P-value < 0.05 was established as the statistically significant difference between groups.

RESULTS

Histopathological findings (Figs. 1A-D). The histological structure of the renal parenchyma (glomeruli and tubules) in the control and GBL-operated groups of rats was normal. The kidneys of the AMD-intoxicated rats had obvious signs of renal tubular necrosis in their lumens. Examination of rat kidneys that had been orally administered GBL extracts revealed that the renal parenchyma appeared intact.

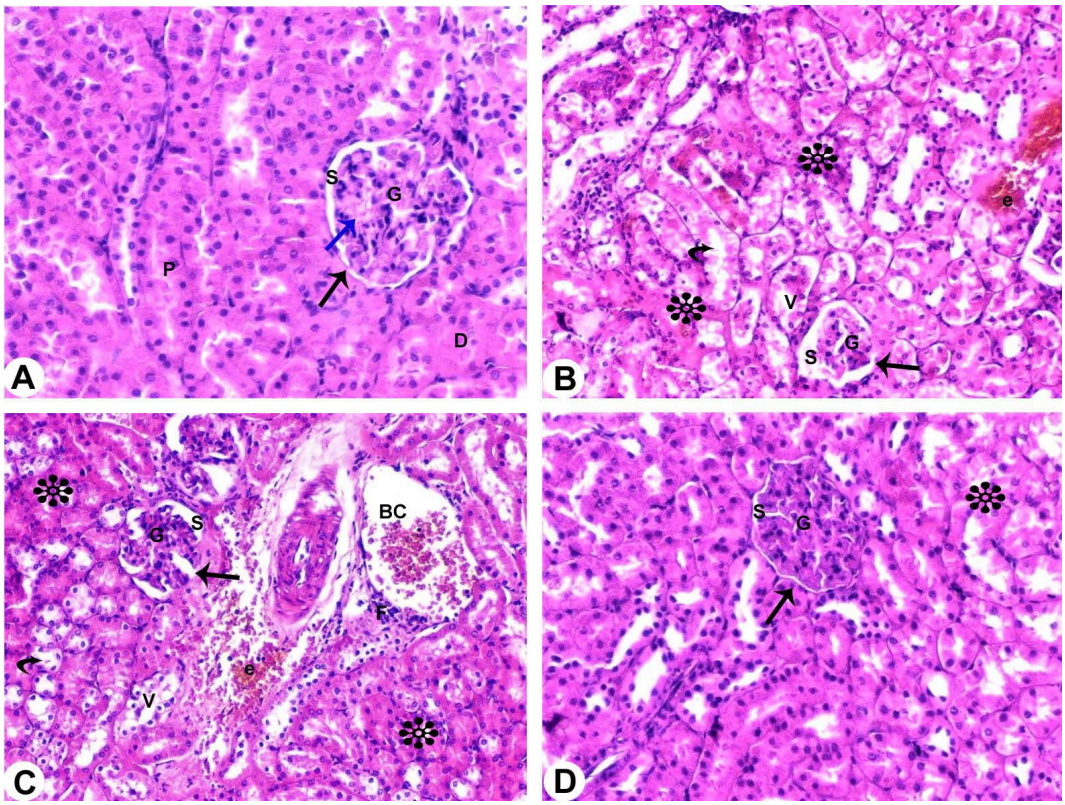

Fig. 1. Photomicrographs of all groups of rat kidneys of the experiment stained with H& E: Bar = 50 µm. **A.** (Groups Control & GBL): a normal architecture of the renal cortex, a renal corpuscle surrounded by proximal (P) and distal (D) convoluted tubules. The renal corpuscle contains the glomerulus (G) and is surrounded by Bowman's capsule. The parietal layer of glomerular capsule (Bowman's capsule) is formed of simple squamous epithelium (black arrow), while the visceral layer is formed of podocytes (blue arrow) with capsular space (Bowman's space) in between (s). **B.** (AMD group): A distorted architecture of the renal cortex; shrunken glomerulus (G), wide Bowman's space (s), discontinuity of glomerular capsule (black arrow). Some renal corpuscles have capsular adhesions with the glomerulus (asterisks). There is also loss of tubular epithelium (curved arrow), sloughing into the lumen, vacuolation (V), and extravasation (e). **C.** (AMD group): A distorted architecture of the renal cortex; shrunken glomerulus (G), wide capsular space (s), discontinuity of glomerular capsule (black arrow). Some renal corpuscles have capsular adhesions with the glomerulus (asterisks) and congested capillaries (BC). There is also loss of tubular epithelium (curved arrow), sloughing into the lumen, vacuolation (V), extravasation (e) and inflammatory cells infiltration (F). **D.** (GBL plus AMD group): A nearly normal glomerulus (G) and capsular space (s), and few adhesions (asterisk) compared to control group.

Normal renal corpuscles, proximal (PT) and distal (DT) convoluted tubules, and a small proportion of the interstitial tissue typical of normal renal architecture were visible in sections from the control and sham-operated animals. The glomerulus corpuscle was encased in a glomerular capsule (Bowman's capsule), which had a visceral layer lined by podocytes and an exterior layer of simple squamous epithelium. Capsular space (Bowman's space) stood between the two strata. The PT had an acidophilic, high cubical cell lining and a restricted lumen, whereas the DT had a large lumen and a pale cubical epithelial lining.

The AMD group showed a marked distortion of renal cortical architecture. Most of the glomeruli were significantly shrunken and destroyed, and the glomerular capsule appeared to widen. Interstitial blood vessels and glomerular capillaries were congested and dilated. Some of the renal corpuscles had ruptured the glomerular capsule, while others showed capsular adhesions. Most of the PT and DT were destroyed and disorganized with the loss of cellular architecture. In some tubules, the epithelial lining had been lost, while in others, the cells exhibited vacuolated cytoplasm and pyknotic nuclei. Cell sloughing was visible in several tubules' lumina.

GBL plus AMD group showed fewer histopathological changes compared to the AMD group. The PT and DT had some areas of loss of cellular architecture.

Ultrastructural observations. The kidneys of control and sham-operated groups displayed a glomerulus with its capillary lumen, a basement membrane, endothelial cells, and visceral epithelial cells with foot processes. The glomerular basement membrane has three layers: an inner one (Lamina rara interna), an exterior one (Lamina rara externa), and a dense center one (Lamina densa). Thin diaphragms, several fenestrates, foot processes, and capillary lumen were observed. The PT images showed epithelial cells lying on a basement membrane, multiple mitochondria, a round nucleus, and long microvilli with brush-like edges on their apical surfaces. Short microvilli, a circular nucleus, a lumen, some epithelial cells sitting on the basement membrane, and some epithelial cells were seen on DT (Figs. 2A-D).

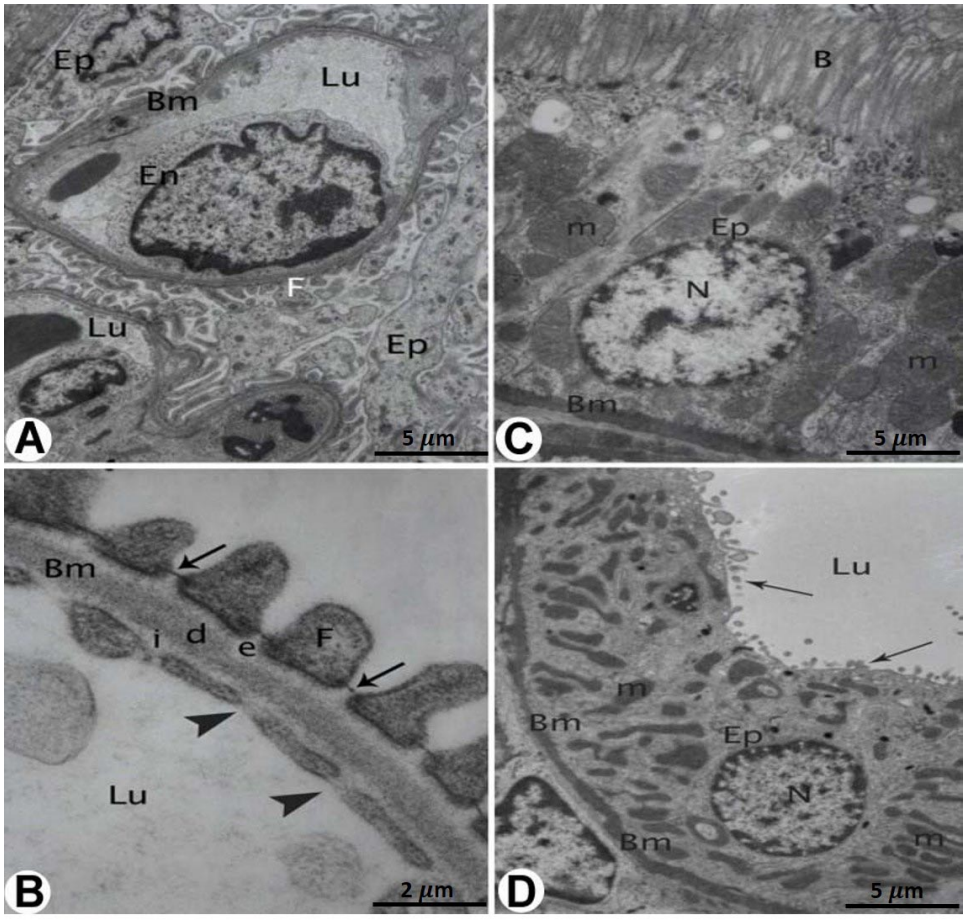

Fig. 2. Electron photomicrographs of group I and II kidney: Bar = 2 & 5 µm. **A.** A glomerulus showing its capillary Lumen (Lu), a basement membrane (BM), endothelial cell (En) and a visceral epithelial cell (Ep) with foot processes (F). **B.** A higher magnification of figure A showing the three layers of the glomerular basement membrane (Bm); its inner (Lamina rara interna, i), its outer (Lamina rara externa, e), and a dense central one (the lamina densa, d). Thin diaphragms (arrows), multiple fenestrate (Arrowhead), foot processes (F) and capillary lumen (Lu) are also seen. **C.** A proximal convoluted tubule showing epithelial cells (Ep) resting on a basement membrane (Bm) withnumerous mitochondria (m) and a round nucleus (N). Its apical surface shows long microvilli of a brush border (B). **D.** A distal convoluted tubule showing some epithelial cells (Ep) resting on the basement membrane (Bm), short microvilli (arrows), a round nucleus (N), mitochondria (m) and lumen (Lu).

Rats treated with AMD were observed in electron photomicrographs to have glomerular capillary basement membranes with two hump-like deposits, a few membrane branches extending to the glomerular lumen, and endothelial cells with pyknotic nuclei. A glomerular capillary showed a focal thickening of its basement membrane with few intramembranous immune deposits. An endothelial cell showed a damaged membrane and mitochondria and its nucleus with a heterochromatin and a vacuole with myelin figure in its lumen were seen. Subendothelial immune deposits in a glomerular capillary with obstructed lumen were demonstrated. In the cytoplasm of epithelial cells, electron dense deposits, foot processes fusion, and a thicker basement membrane were seen (Figs. 3A-E).

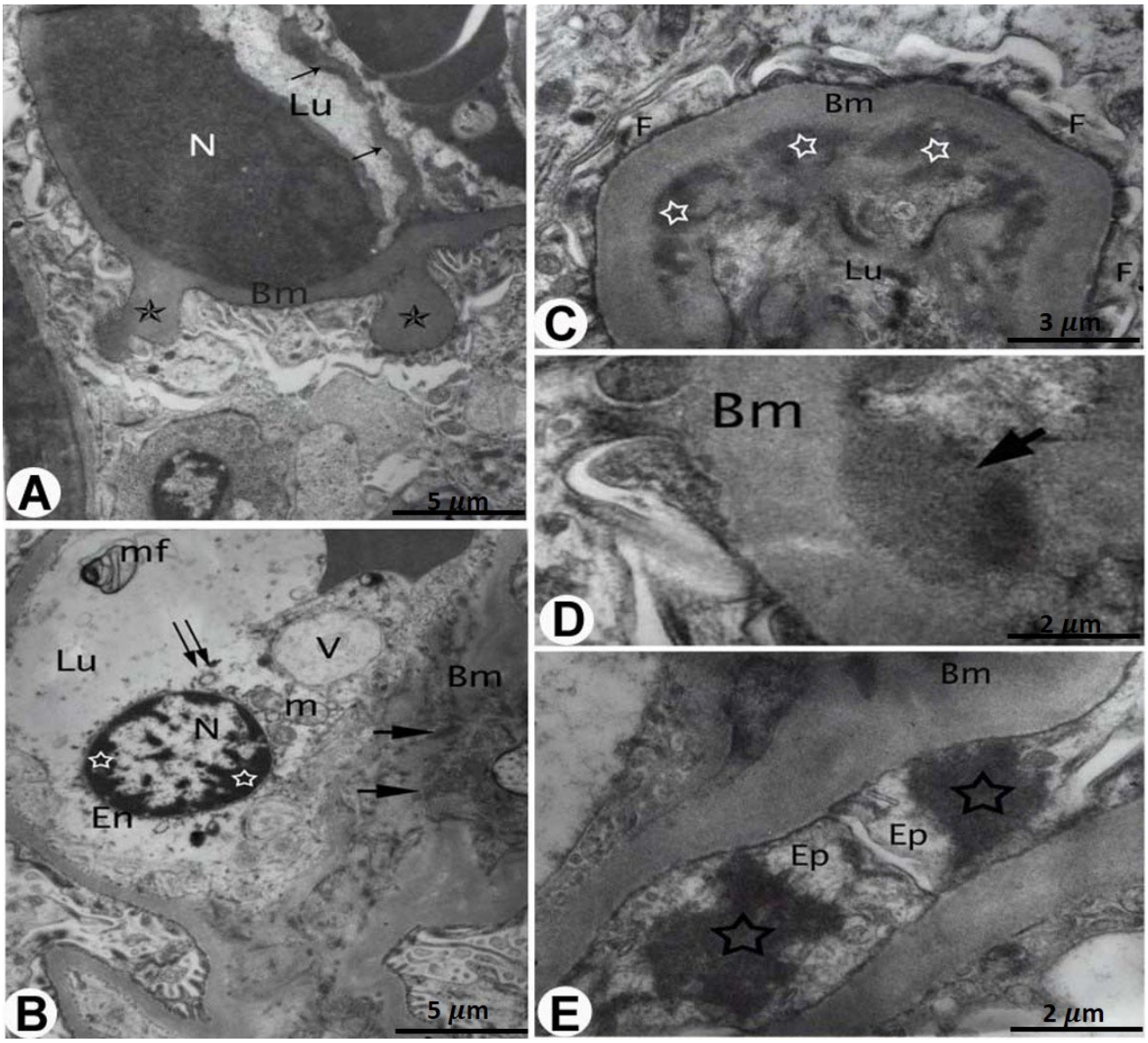

Fig. 3. Electron photomicrographs of AMD–treated rats: Bar = 2 & 3 &5 μm. **A.** A glomerular capillary basement membrane (Bm) showing two hump-like deposits (Stars). A few branches of membranes (arrows) extend from basement membrane to the glomerular lumen (Lu). A pyknotic nucleus (N) of the endothelial cell is also seen. **B.** A glomerular capillary showing a focal thickening of its basement membrane (Bm) with few intramembranous immune deposits (arrows). An endothelial cell (En) showing a damaged membrane (double arrows) and mitochondria (m) and its nucleus (N) with a heterochromatin (Stars) and a vacuole (V) with myelin figure (mf) in its lumen (Lu) are also seen. **C&D.** Subendothelial immune deposits (arrows) in a glomerular capillary with obstructed its lumen (Lu) are demonstrated. Foot processes fusion (F) and a basement membrane (Bm) are also seen. **E.** Electron dense deposits (stars) are seen inside epithelial cell (Ep) cytoplasm. A thickened basement membrane (Bm) of a glomerular capillary is also seen.

PT showed a loss of epithelial cell boundaries and basal infoldings, its cytoplasm showed a scattered damaged mitochondria and vacuoles. A basement membrane and a nucleus were seen. PT showed a degenerated epithelial cell cytoplasm, large lipid droplets and a degenerated nucleus. Damaged microvilli and loss of basal Infoldings were also seen. The PT image revealed a degraded epithelial cell with a damaged nucleus, mitochondria, and cytoplasm, as well as focal microvilli destruction. Blebs were seen in its lumen. DT illustrated swollen epithelial cells with bleb formation and loss of its microvilli (Figs. 4A-D).

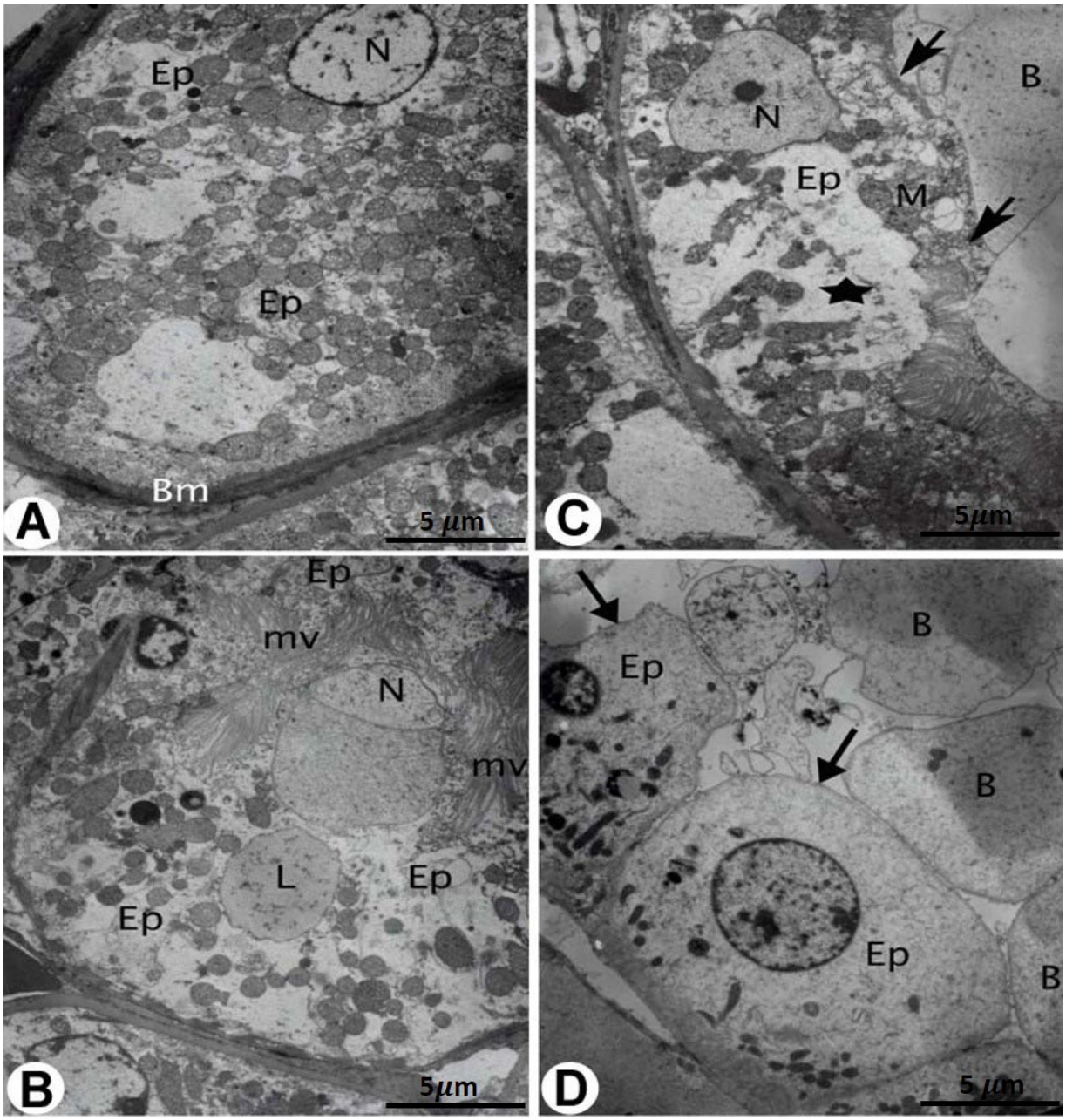

Fig. 4. Electron photomicrographs of AMD–treated rats: Bar = 5 μm. **A.** A proximal convoluted tubule showing a loss of epithelial cell (Ep) boundaries and basal infoldings, its cytoplasm showing a scattered damaged mitochondria and vacuoles (V). A basement membrane (Bm) and a nucleus (N) are also seen. **B.** A proximal convoluted tubule showing a degenerated epithelial cell (Ep) cytoplasm, large lipid droplets (L) and a degenerated nucleus (N). Damaged microvilli (mv) and disappearance of basal Infoldings are also seen. **C.** A proximal convoluted tubule showing a degenerated epithelial cell (Ep) with damaged nucleus (N), mitochondria (M) and cytoplasm (star) as well as focal destruction of microvilli (arrows). Blebs (B) are seen in its lumen. **D.** A distal convoluted tubule illustrating swollen epithelial cells (Ep) with bleb (B) formation and disappearance of its microvilli (arrows).

Rats given the AMD and GBL treatments exhibited intact basement membranes in the glomeruli and visceral epithelial cells with fusedfocal foot processes. A few glomerular basement membrane wrinkles with intact epithelial cells and irregular-shaped nucleus were seen. PT showed healthy mitochondria, many lysosomes, nucleus, and brush border microvilli. Loss of basal Infoldings was also seen. DT demonstrated minimal changes in microvilli, epithelial cell nucleus and basal infoldings (Figs. 5A-D).

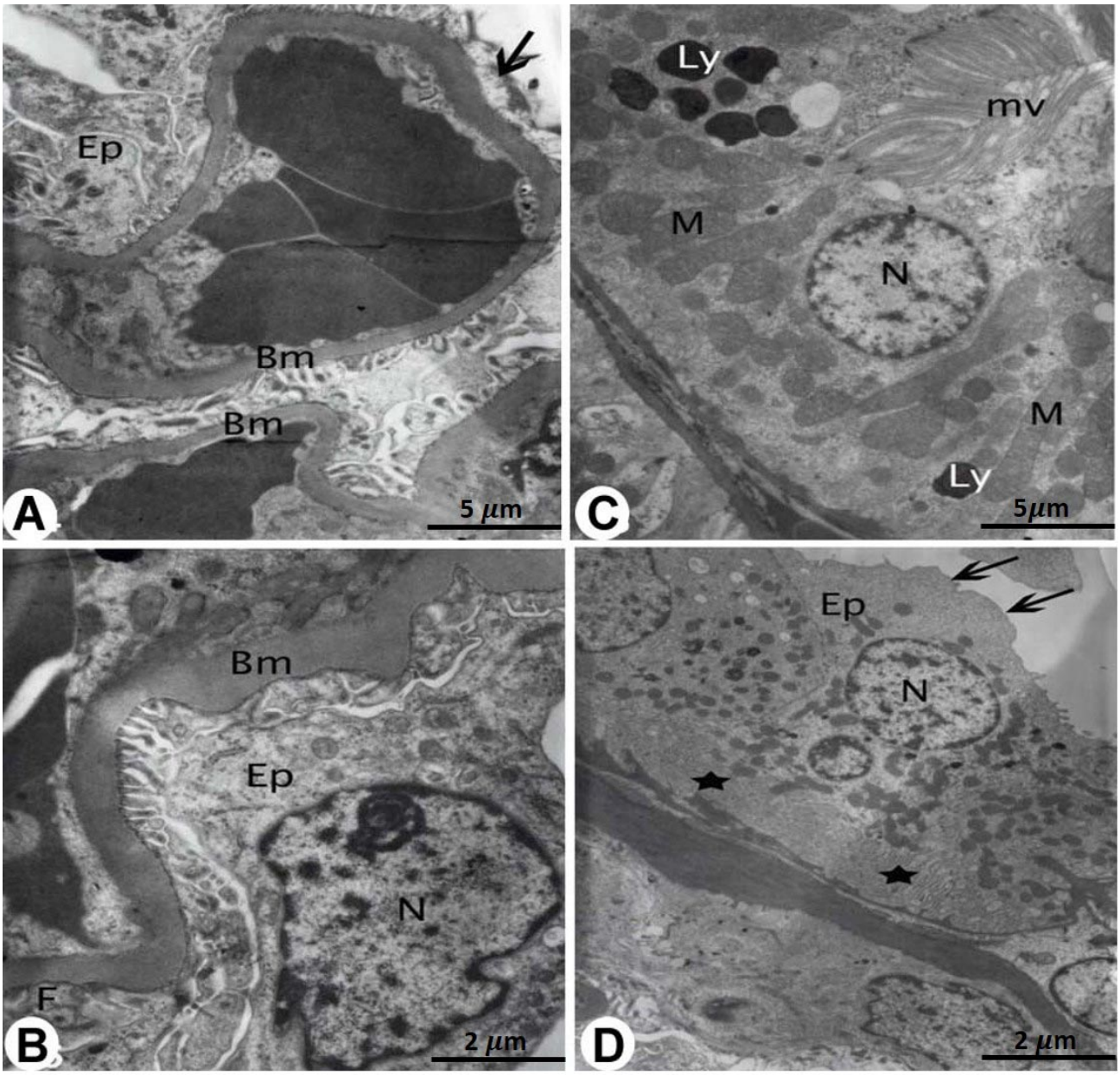

Fig. 5. Electron photomicrographs of GBL plus AMD treated rats: Bar = 2 & 5 μm. **A.** A glomerulus showing intact basement membrane (Bm) and visceral epithelial cells (Ep) with focal footprocesses fusion (arrow). **B.** A few wrinkling of glomerular basement membrane (Bm) and intact epithelial cell (Ep) with irregular-shaped nucleus (N) are seen. Focal foot processes fusion (F) is also seen. **C.** A proximal convoluted tubule showing intact mitochondria (M), multiple lysosomes (Ly), nucleus (N) and brush border microvilli (mv). Disappearance of basal Infoldings is also seen. **D.** A distal convoluted tubule demonstrating minimal changes in microvilli (arrows), epithelial cells (Ep) nucleus (N) and basal infoldings (star).

Biochemical findings.

Renal functional markers. Acute renal impairment caused by AMD injection was demonstrated by an increase in urea (Fig. 6A), creatinine (Fig. 6A), and protein excretion rate (Fig. 7B) as compared to the control group. However, urea, creatinine, and protein excretion levels significantly decreased after GBL therapy compared to the AMD group. Measurements of Urinary NAG. Rats' urine N-acetyl-b-D-glycosaminidase (NAG) levels significantly increased with AMD compared to control group rats was observed. Additionally, the urine NAG level has significantly decreased in the GBL + AMD group (Fig. 7).

Oxidative stress biomarkers. In the kidney homogenates of AMD-treated animals, MDA concentrations (Fig. 8A) significantly increased when compared to controls. Treatment with GBL could reduce renal MDA concentrations in the treated group in comparison with the AMD group. In the GBL plus AMD group, MDA level regenerated close to normal concentration in the control group.

GPx activities in the kidney are indicated in Figure 8B. The induction of AMD nephrotoxicity was accompanied by a significant decrease in renal GPX activity in comparison with the control group. GBL treatment returned renal GPX activity close to control levels.

AMD nephrotoxicity considerably reduced the renal activities of CAT in comparison to the control group (Fig. 8C). GBL treatment considerably recovered renal CAT activity to normal levels observed in controls.

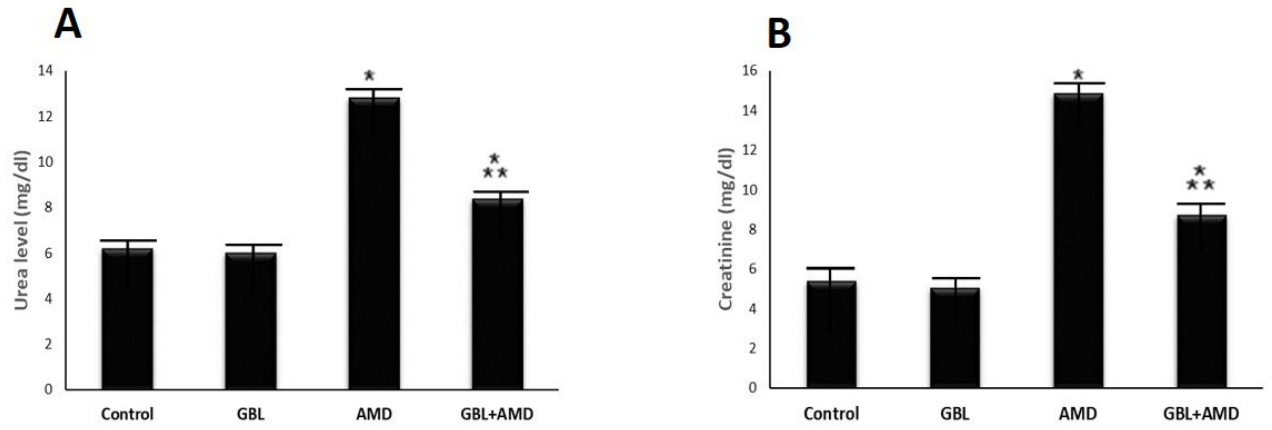

Fig. 6. The effects of GBL extract administration on renal functional parameters including urea (A) and creatinine (B) in AMD nephrotoxicity. Data are represented as Mean ± SD (n=6). One-way ANOVA followed by a post hoc LSD test was used for comparison between different groups. *Significant change in comparison with the control group at $P < 0.05$; Significant change in comparison with the AMD group at $P < 0.05$

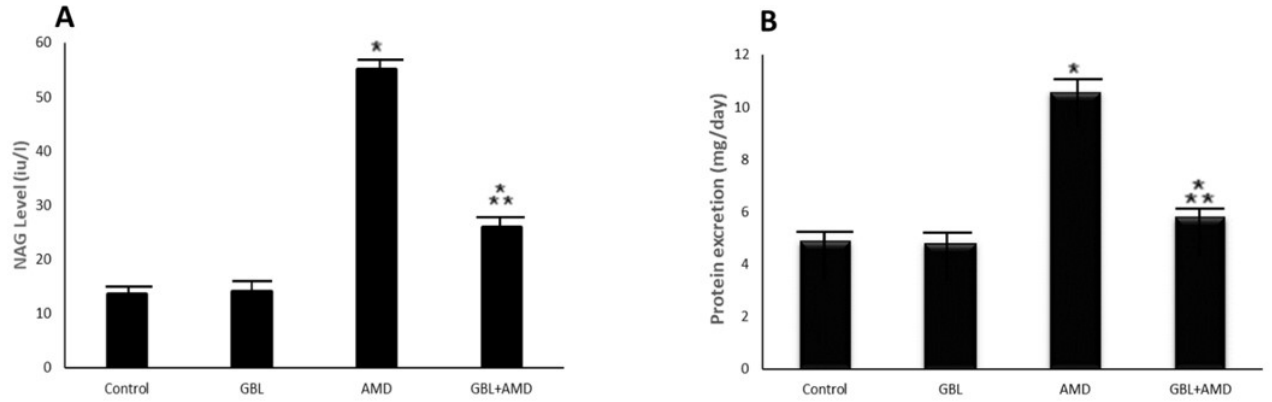

Fig. 7. The effects of GBL extract administration on renal functional parameters including Urinary N-acetyl-b-D-glucosaminidase (NAG) activity (A) and protein excretion rate (B) in AMD nephrotoxicity. Data are represented as Mean ± SD (n=6). One-way ANOVA followed by a post hoc LSD test was used for comparison between different groups. *Significant change in comparison with the control group at $P < 0.05$; Significant change in comparison with the AMD group at $P < 0.05$

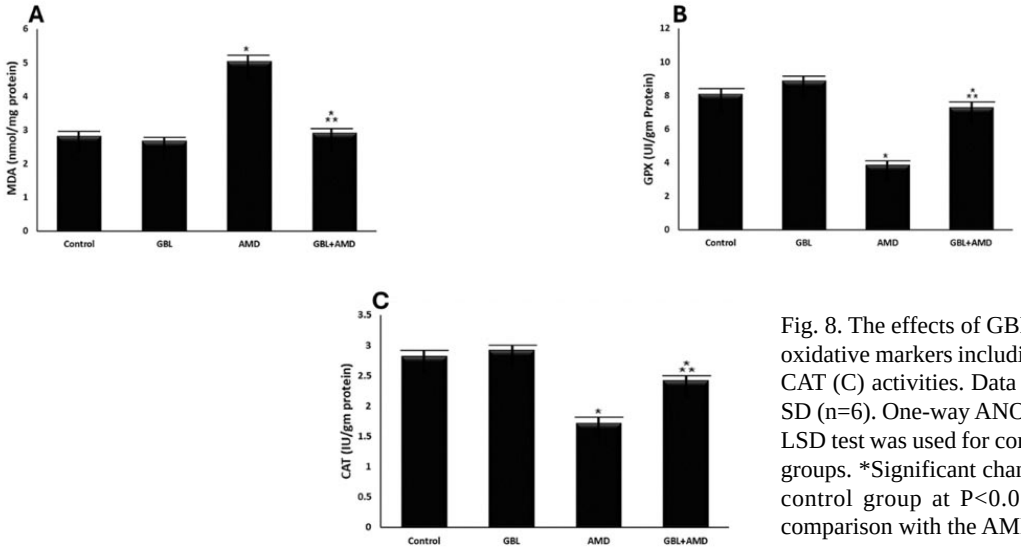

Fig. 8. The effects of GBL extract administration on oxidative markers including MDA (A), GPx (B) and CAT (C) activities. Data are represented as Mean ± SD (n=6). One-way ANOVA followed by a post hoc LSD test was used for comparison between different groups. *Significant change in comparison with the control group at P<0.05; Significant change in comparison with the AMD group at P < 0.05

DISCUSSION

AMD is a frequently used, effective treatment for atrial fibrillation, atrial flutter, ventricular arrhythmias, and supraventricular tachycardia (Istratoaie *et al*., 2021). However, AMD medication resulted in severe adverse effects that were time and dose dependent. Several plants, plant extracts, or plant derivatives are now frequently utilized for disease prevention and treatment. GBL extract exhibited remarkable antioxidant effects (Pandita *et al*., 2021). To determine whether GBL could protect the kidneys against AMD in rats, this study set out to examine that possibility.

The histological alterations in the kidneys showed tissue injury upon AMD treatment along with degenerative impairments to its structure. In addition, kidney tissue showed morphological abnormalities in AMD-treated rats as opposed to controls. Bowman's space enlargement, glomerulus hypercellularity, and PT's epithelial cell degenerative changes were all brought on by AMD. The renal damage triggered by AMD in rats was validated by these data, which coincide with studies that showed a tubular change in renal tissue linked with AMD therapy in comparison with controls (Sakr & El-Gamal, 2016; Torimitsu *et al*., 2022). It has been demonstrated that AMD alters the kidney's histoarchiterural structure and increases cytokine production (Chakraborty *et al*., 2014; Ashkar *et al*., 2022).

It is interesting that we observed capsular adhesions, also known as glomerular tip adhesions or the glomerular capsule adhesions, in the AMD group. These are characterized as a continuity of the extracellular matrix of the glomerulus and capsular outer layer (Bowman's parietal layer) (Selamet *et al*., 2020). Capillaries and the associated podocytes move peripherally, adhere to the parietal epithelium, and create a tight junction, which is how capsular adhesions are explained (Jennings *et al*., 2023).

The majority of AMD group's PT and DT were damaged, disordered, and lost their cellular architecture. While some tubules possessed vacuolated cytoplasm and pyknotic nuclei, others displayed cellular sloughing with focal loss of its microvilli. PT cells had electron-dense broken mitochondria, rarefied vacuolated cytoplasm, fragmented microvilli, and lysosome remnants. The nuclei exhibited discontinuous nuclear membranes were smaller than usual, and apically displaced (Lin *et al*., 2020; Jennings *et al*., 2023).

The findings were explained by a decline in renal tubule reabsorption caused by AMD, atrophy of the glomeruli, which reduces glomerular filtration, and degradation of tubular epithelial cells (Meng *et al*., 2021). Oxidative damage is prompted by AMD-induced toxicity, which is triggered by the creation of ROS. Our findings are consistent with previous observations that AMD causes antioxidant enzyme depletion, which leads to oxidative stress and cytotoxicity (Hadrava Vanova *et al*., 2020).

A possible explanation for the renal oxidative stress brought on by AMD is that the disease increased the production of hydrogen peroxide in mitochondria, which led to peroxidation (Betiu *et al*., 2021). Furthermore, AMD medication caused an increase in urinary iodine, hypertrophied brain, and cortisol levels. An increase in lipid peroxidation created stress for the deiodination process and the AMD metabolism, which led to renal damage (Torimitsu *et al*., 2022). As part of the pathophysiology of its toxicity,

AMD can produce free radicals, hinder phospholipases, and destabilize membranes (Tsukimura *et al*., 2021; Sagini *et al*., 2021). Additionally, AMD after metabolism releases extra iodine into the blood when it is deionized, which causes oxidative stress and free radicals to form in the kidney and liver (Ashkar *et al*., 2022, Essrani *et al*., 2020). The kidneys are vulnerable to injury due to the injection of AMD, which leads to higher quantities of discharged chemicals and peritubular cell perfusion (Sakr & El-Gamal, 2016; Miano *et al*., 2020).

Serum creatinine and urea levels were measured as part of this investigation to assess renal function. The serum levels of creatinine and urea are reported to increase after AMD treatment, indicating a decline in kidney function. The AMD-induced nephrotoxicity, which manifests as an impairment in glomerular filtration rate and direct tubular injury, may also be responsible for these consequences (Thind *et al*., 2022; Vamos *et al*., 2022).

Biochemical analysis showed that renal MDA concentration significantly enhanced in AMD-treated animals compared with controls. The current study suggested that cell membrane lipids were exposed to ROS attacks as a result of an increase in MDA in the kidney tissues of the AMD group (Belhadj Slimen *et al*., 2014). The MDA was one of the end products of lipid peroxidation and was frequently used to determine whether or not oxidative stress was experienced (Bedir *et al*., 2023).

The CAT activity was suppressed in the AMD group according to experimental results. In this study, CAT was evaluated as another indicator of antioxidant activity. The CAT was a key enzyme in the detoxification of H2O2. As CAT activity decreased, the amount of H2O2 in the body increased, which caused both direct damage to cells and the Fenton reaction to damage them as well (Wang *et al*., 2018). Like current findings. AMD reduced CAT activity in kidney tissues (Sndos & Al-Amri, 2019).

The GPx activity was reduced in the AMD group according to our results. GPX enzyme system is essential for normal intracellular homeostasis and gets disturbed under pathophysiologic conditions including endothelial dysfunction (Panday *et al*., 2020).

GBL is one of the most widely used phytotherapeutic products in the world, and its extract has beneficial properties for the treatment ofseveral pathologies. GBL can be a low-cost alternative to the therapeutic approach of several pathologies since it acts in the prevention, treatment, and inhibition of several complications of common comorbidities (de Souza *et al*., 2020).

On the other hand, several studies determined that AMD decreased the activities of antioxidant enzymes which are in accordance with our study. GBL administration could reduce MDA concentration in the treated group. Moreover, these extracts have been found to ameliorate renal ischemia-reperfusion injury, chronic kidney disease, and hypertension-induced renal injury. They achieve this by reducing tissue damage, inhibiting vascular smooth muscle cell calcification induced by b-glycerophosphate, and enhancing the effects of losartan on reducing renal tissue oxidative stress (Wang *et al*., 2019).

In addition, GBL clearly recovered the renal activities of CAT and GPX in AMD treated animals of this study. When GBL and AMD were given together in the current investigation, the kidney tissues showed a notable improvement when compared to the AMD group. Natural antioxidant molecules have garnered more attention recently as a means of lowering drug-induced nephrotoxicity. In this study, rats given GBL showed noticeably improved defenses against AMD toxicity. These findings supported the GBL extract's nephroprotective properties. With its antioxidant actions, the GBL repaired the oxidative damage. The findings reported were consistent with several studies that showed GBL extract improved kidney function in a model of diabetic nephropathy (Lu *et al*., 2015), as well as Adriamycin (Abd-Ellah & Mariee, 2007), methotrexate (Tousson *et al*., 2014), and cisplatin (Song *et al*., 2013)-induced renal toxicity models. This impact could be explained by the fact that GBL contains a number of naturally occurring chemicals that control the equilibrium between antioxidants and oxidants (Tousson *et al*., 2014).

In addition, GBL extract showed cytoprotective qualities against apoptosis and oxidative damage, according to (Biernacka *et al*., 2023). The GBL extract contains numerous antioxidant components, including flavonoids, diterpene terpenoids, catechins, steroids, quercetin, kaempferol, flavone glycosides, and others (Razná *et al*., 2020; Su *et al*., 2022). Additionally, GBL extract includes proanthocyanidins and flavonol glycosides, which have antioxidant and free radical scavenging activities, preventing and treating a number of disorders brought on by oxidative damage (Samec *et al*., 2022).

The obtained results were in harmony with several researches that revealed amelioration of kidney function with GBL extract in diabetic nephropathy model (Lu *et al*., 2015), as well as Adriamycin (Abd-Ellah & Mariee, 2007), methotrexate (Tousson *et al*., 2014), and cisplatin (Song *et al*., 2013)-induced renal toxicity models. This effect could be explained through GBL containing several natural

compounds that regulate the balance between the antioxidants and oxidants (Tousson *et al*., 2014). Moreover, Hsu *et al*. (Hsu *et al*., 2009) reported that GBL extract had therapeutic mechanisms and cytoprotective effects against apoptosis and oxidative damage. There are many antioxidant constituents in GBL extract like flavonoids, diterpene terpenoids, catechins, steroids, quercetin, kaempferol, flavone glycosides, etc. (Vasseur *et al*., 1994, Brown, 1996). Moreover, GBL extract contains proanthocyanidins and flavonol glycosides, which have antioxidant and free radical scavenging properties, thus protecting and improving many diseases resulting from oxidative damage (Joyeux *et al*., 1995).

However, the significant reduction in urea and creatinine levels observed once GBL was administered along with AMD suggested that GBL had protective benefits. This can be explained by beneficial and antioxidant effects of GBL (Du *et al*., 2019).

In the current study, rats given AMD experienced large increases in urine NAG levels, which GBL extract was able to lower. Abnormal urinary NAG excretion has been linked to a variety of renal disorders, including nephrotic syndrome, glomerulonephritis, urinary tract infection, vesicoureteral reflux, acute kidney injury, hypertension, drug nephrotoxicity, and renal allograft rejection (Mohkam & Ghafari, 2015; Sagini *et al*., 2021).

CONCLUSION

AMD led to a decrease in antioxidants in the renal tissues of rats as well as an increase in oxidants and kidney function tests. Proinflammatory cytokines were increased, suggesting that AMD harm was also mediated by inflammatory mechanisms. The harmful effects of AMD on kidney tissue were verified by histopathological studies. GBL, However, demonstrated anti-inflammatory and antioxidant activities that shielded kidney tissue from AMD's effects. Molecular research should be conducted to gain a deeper comprehension of the toxic effects of AMD on kidney tissue as well as the mechanism underlying the protective benefits of GBL.

ACKNOWLEDGEMENTS

The authors extend their appreciation to the Deanship of Research and Graduate Studies at King Khalid University for funding this work through Research Project under grant number RGP2/112/46. Also, the researchers would like to thank the Deanship of Scientific Research at King Faisal University for providing the funding for publishing this research.

DAWOOD, S. A.; EID, R. A.; ABADI, A. M.; SHATI, A. A.; JAMIL, S.; EL-KOTT, A. F.; MOHAMED, G.; AL-SHRAIM, M.; HAMAD, Y. A.; SALIH, A. G. A.; ALARABI, T. G. M.; AL-HAIDER, S. M.; ALYAMI , E. M. & ZAKI, M. S. A. Efecto protector renal del extracto de *Ginkgo biloba* frente a la toxicidad inducida por amiodarona, el estrés oxidativo y las lesiones. *Int. J. Morphol., 43(6)*:1843-1856, 2025.

RESUMEN: La amiodarona (AMD) se clasifica como un antiarrítmico. Los efectos secundarios graves del tratamiento incluyeron una reducción significativa de la función renal. El extracto de hojas de *Ginkgo biloba* (GBL) ha demostrado ser un eficaz eliminador de radicales libres y antioxidante. El propósito de este estudio fue evaluar el efecto del extracto de GBL sobre la nefrotoxicidad inducida por la AMD. Cuarenta ratas macho se dividieron en cuatro grupos. Grupo I Control. Grupo II recibió extracto de GBL. El día 21, el grupo AMD recibió una inyección intraperitoneal (i.p.) de AMD. En el grupo GBL más AMD, las ratas recibieron GBL durante 21 días antes de recibir AMD. Después de cuatro semanas, las ratas fueron sacrificadas y se les extirparon los riñones para determinar los niveles histológicos y ultraes-tructurales de N-acetil-beta-D glicosaminidasa (NAG), marcadores de función renal como urea sérica, creatinina, tasa de excreción de proteínas, citocinas inflamatorias y marcadores de estrés oxidativo. El daño renal inducido por la DMAE en ratas puede ser provocado por estrés oxidativo, que produce una citotoxicidad renal significativa, como lo demuestran las investigaciones bioquímicas, histopatológicas y de microscopía electrónica. Tras la administración de extracto de GBL al grupo con DMAE, todos los parámetros analizados en este estudio mejoraron significativamente. Según los hallazgos del presente estudio, el extracto de GBL redujo la nefrotoxicidad inducida por la DMAE al actuar como antioxidante.

PALABRAS CLAVE: Amiodarona; Nefrotoxicidad; Ginkgo biloba; Histopatología; Marcadores de función renal; NAG.

REFERENCES

Abd-Ellah, M. F. & Mariee, A. D. *Ginkgo biloba* leaf extract (EGb 761) diminishes adriamycin-induced hyperlipidaemic nephrotoxicity in rats: association with nitric oxide production. *Biotechnol. Appl. Biochem., 46*:35-40, 2007.

Ashkar, F.; Bhullar, K. S. & Wu, J. The effect of polyphenols on kidney disease: targeting mitochondria. *Nutrients, 14(15)*:3115, 2022.

Bedir, Z.; Erdem, K.; Can, A.; Çiçek, B.; Güliboglu, M.; Süleyman, Z.; Gürsul, C.; Mokhtare, B.; Özçiçek, F. & Süleyman, H. Effect of thiamine pyrophosphate upon possible metamizole-induced liver injury in rats. *Int. J. Pharmacol., 19*, 2023.

Behl, T.; Kaur, G.; Sehgal, A.; Zengin, G.; Singh, S.; Ahmadi, A. & Bungau, S. Flavonoids, the family of plant-derived antioxidants making inroads into novel therapeutic design against ionizing radiation-induced oxidative stress in Parkinson's disease. *Curr. Neuropharmacol., 20(2)*:324-43, 2022.

Belhadj Slimen, I.; Najar, T.; Ghram, A.; Dabbebi, H.; Ben Mrad, M. & Abdrabbah, M. Reactive oxygen species, heat stress and oxidative-induced mitochondrial damage: a review. *Int. J. Hyperthermia, 30(7)*:513-23, 2014.

Betiu, A. M.; Chamkha, I.; Gustafsson, E.; Meijer, E.; Avram, V. F.; Åsander Frostner, E.; Ehinger, J. K.; Petrescu, L.; Muntean, D. M. & Elmér, E. Cell-permeable succinate rescues mitochondrial respiration in cellular models of amiodarone toxicity. *Int. J. Mol. Sci., 22(1)*:11786, 2021.

Biernacka, P.; Adamska, I. & Felisiak, K. The potential of *Ginkgo biloba* as a source of biologically active compounds: a review of the recent literature and patents. *Molecules, 28(10)*:3993, 2023.

Brown, D. Phytotherapy: herbal medicine meets clinical science. *NARD J., 118*:41-52, 1996.

Chakraborty, A.; Mondal, C.; Sinha, S.; Mandal, J. & Chandra, A. K. Amiodarone-induced oxidative stress in stress-vulnerable organs of adult male rats. *Asian J. Pharm. Clin. Res., 7*:177-83, 2014.

Çuhadar, S. & Semerci, T. Renal biomarkers N-acetyl-b-D-glucosaminidase (NAG), endothelin, and their application. *Biomark. Kidney Dis.*, 369-96, 2016.

Cui, J.; Hu, L. A.; Shi, W.; Cui, G.; Zhang, X. & Zhang, Q.-W. Phytochemical analysis and bioactivity of natural compounds. *Molecules, 24(11)*:2156, 2019.

Das, S.; Vasudeva, N. & Sharma, S. Pharmacognostical evaluation of *Tribulus terrestris* L. *Int. J. Pharm. Sci. Res., 8(3)*:393-400, 2017.

de Souza, G. A.; de Marqui, S. V.; Matias, J. N.; Guiguer, E. L. & Barbalho, S. M. Effects of *Ginkgo biloba* on diseases related to oxidative stress. *Planta Med., 86*:376-86, 2020.

Deng, J.; Gan, Y.; Shan, Y. & Guo, H. Comparison of radiofrequency ablation and antiarrhythmic drug for the treatment of atrial fibrillation: a protocol for systematic review and meta-analysis. *Medicine (Baltimore), 101(51)*:e32184, 2022.

Du, Y.; Xu, B. J.; Deng, X.; Wu, X. W.; Li, Y. J.; Wang, S. R.; Wang, Y. N.; Ji, S.; Guo, M. Z.; Yang, D. Z. & Tang, D. Q. A sensitive and robust HILIC-MS/MS method for the determination of plasma free amino acids and its application to type 2 diabetes mellitus research. *J. Pharm. Biomed. Anal., 166*:30-9, 2019.

Ebeid, W. M.; El-Shazly, A. A. E.-F.; Kamal, N. M.; Fakhary, E. E.; Mansour, A. & Ashour, D. M. New insights into amiodarone-induced retinal and optic nerve toxicity: functional and structural changes. *Ther. Adv. Ophthalmol., 15*:25158414231194159, 2023.

Essrani, R.; Mehershahi, S.; Essrani, R. K.; Ravi, S. J. K.; Bhura, S.; Sudhakaran, A.; Hossain, M. & Mehmood, A. Amiodarone-induced acute liver injury. *Case Rep. Gastroenterol., 14(1)*:87-90, 2020.

Fang, C.-Y.; Lou, D.-Y.; Zhou, L.-Q.; Wang, J.-C.; Yang, B.; He, Q.-J.; Wang, J.-J. & Weng, Q.-J. Natural products: potential treatments for cisplatin-induced nephrotoxicity. *Acta Pharmacol. Sin., 42(2)*:1951-69, 2021.

Gray, M. P.; Barreto, E. F.; Schreier, D. J.; Kellum, J. A.; Suh, K.; Kashani, K. B.; Rule, A. D. & Kane-Gill, S. L. Consensus obtained for the nephrotoxic potential of 167 drugs in adult critically ill patients using a modified Delphi method. *Drug Saf., 45(4)*:389-98, 2022.

Hadrava Vanova, K.; Kraus, M.; Neuzil, J. & Rohlena, J. Mitochondrial complex II and reactive oxygen species in disease and therapy. *Redox Rep., 25(1)*:26-32, 2020.

Hsu, C.-L.; Wu, Y.-L.; Tang, G.-J.; Lee, T.-S. & Kou, Y. R. *Ginkgo biloba* extract attenuates cigarette smoke-induced lung inflammation by inhibiting NF-kB activation in rats. *Pulm. Pharmacol. Ther., 22*:286-96, 2009.

Istratoaie, S.; Sabin, O.; Vesa, S. C.; Cismaru, G.; Donca, V. I. & Buzoianu, A. D. Efficacy of amiodarone for the prevention of atrial fibrillation recurrence after cardioversion. *Cardiovasc. J. Afr., 32(6)*:327-38, 2021.

Jennings, P.; Carta, G.; Singh, P.; da Costa Pereira, D.; Feher, A.; Dinnyes, A.; Exner, T. E. & Wilmes, A. Capturing time-dependent activation of genes and stress-response pathways using transcriptomics in iPSC-derived renal proximal tubule cells. *Cell Biol. Toxicol., 39*:1773-93, 2023.

Joyeux, M.; Lobstein, A.; Anton, R. & Mortier, F. Comparative antilipoperoxidant, antinecrotic and scavenging properties of terpenes and biflavones from Ginkgo and some flavonoids. *Planta Med., 61(2)*:126-9, 1995.

Lan, P.; Kang, D.; Mii, A.; Endo, Y.; Tagawa, M.; Yu, X.; Lyu, J.; Xie, L.; Shimizu, A. & Terasaki, M. Hyaline arteriolosclerosis-associated paratubular basement membrane insudative lesions in distal renal tubules. *Clin. Exp. Nephrol., 26*:216-25, 2022.

Li, D.; Li, Y.; Yang, S.; Yu, Z.; Xing, Y. & Wu, M. Protective effects and mechanisms of *Ginkgo biloba* extract on kidney injury: a review. *Front. Pharmacol., 13*:811422, 2022.

Lin, N.; Zhou, X.; Geng, X.; Drewell, C.; Hübner, J.; Li, Z.; Zhang, Y.; Xue, M.; Marx, U. & Li, B. Repeated dose multi-drug testing using a microfluidic chip-based coculture of human liver and kidney proximal tubule equivalents. *Sci. Rep., 10*:8879, 2020.

Liu, J.; Tang, M.; Li, T.; Su, Z.; Zhu, Z.; Dou, C.; Liu, Y.; Pei, H.; Yang, J.; Ye, H. & Chen, L. Protective effects and mechanisms of *Ginkgo biloba* extract on drug-induced kidney injury. *Front. Pharmacol., 13*:811682, 2022.

Lu, Q.; Zuo, W.-Z.; Ji, X.-J.; Zhou, Y.-X.; Liu, Y.-Q.; Yao, X.-Q.; Zhou, X.-Y.; Liu, Y.-W.; Zhang, F. & Yin, X.-X. *Ginkgo biloba* extract attenuates renal interstitial fibrosis induced by unilateral ureteral obstruction in rats. *Phytomedicine, 22(12)*:1071-8, 2015.

Marin, G. E.; Neag, M. A.; Burlacu, C. C. & Buzoianu, A. D. The protective effects of nutraceutical components in methotrexate-induced toxicity models—an overview. *Microorganisms, 10(10)*:2053, 2022.

Meng, Y.; Wang, S.; Liu, P.; Zhang, Y.; Tang, B.; Zhu, C.; Wang, S.; Yang, Q.; Lu, T. & Nie, C. Amiodarone-induced pulmonary toxicity: clinical features, imaging manifestations, and pathological findings. *J. Thorac. Dis., 13(3)*:1612-23, 2021.

Miano, T. A.; Hennessy, S.; Yang, W.; Dunn, T. G.; Weisman, A. R.; Oniyide, O.; Agyekum, R. S.; Turner,A. P.; Ittner, C. A. G.; Anderson, B. J.; *et al*. Association between nephrotoxic medication burden and acute kidney injury in critically ill adults. *Intensive Care Med., 48(9)*:1144-55, 2022.

Miano, T. A.; Yang, W.; Shashaty, M. G. S.; Zuppa, A.; Brown, J. R. & Hennessy, S. The magnitude of the warfarin–amiodarone drug-drug interaction varies with renal function: a propensity-matched cohort study. *Clin. Pharmacol. Ther., 107(6)*:1446-56, 2020.

Mihoubi, W.; Sahli, E.; Rezgui, F.; Dabebi, N.; Sayehi, R.; Hassairi, H.; Masmoudi-Fourati, N.; Walha, K.; Ben Khadhra, K.; Baklouti, M.; *et al*. Whole and purified aqueous extracts of Nigella sativa L. seeds attenuate apoptosis and the overproduction of reactive oxygen species triggered by p53 over-expression in the yeast Saccharomyces cerevisiae. *Cells, 11(5)*:869, 2022.

Mishra, O. P.; Jain, P.; Srivastava, P. & Prasad, R. Oxidative stress and antioxidant status in children with acute pyelonephritis. *Pediatr. Nephrol., 27*:589-96, 2012.

Mitsa, G.; Guo, Q.; Goncalves, C.; Preston, S. E. J.; Lacasse, V.; Aguilar-Mahecha, A.; Benlimame, N.; Basik, M.; Spatz, A.; Batist, G.; Miller, W. H., Jr.; Del Rincon, S. V.; Zahedi, R. P. & Borchers, C. H. A non-hazardous deparaffinization protocol enables quantitative proteomics of core needle biopsy-sized formalin-fixed and paraffin-embedded (FFPE) tissue specimens. *Int. J. Mol. Sci., 23*:4443, 2022.

Mohkam, M. & Ghafari, A. The role of urinary N-acetyl-b-glucosaminidase in diagnosis of kidney diseases. *J. Pediatr. Nephrol., 3*, 2015.

Morales, A. I.; Barata, J. D.; Bruges, M.; Arévalo, M. A.; González de Buitrago, J. M.; Palma, P.; Branco, P. & Pérez-Barriocanal, F. Protective effect of *Ginkgo biloba* extract against cisplatin-induced nephrotoxicity in rats. *Pharmacol. Toxicol., 92(1)*:39-42, 2003.

Nayok, S. B.; Thimmaiah, S. M. & Dhanashree Akshatha, H. S. Intact higher mental functions despite high serum urea and creatinine levels in a patient with acute kidney injury: a case report. *Indian J. Psychol. Med., 44(2)*:207-8, 2022.

Newman, C.; Price, A.; Davies, D.; Gray, T. & Weetman, A. Amiodarone and the thyroid: a practical guide to the management of thyroid dysfunction induced by amiodarone therapy. *Heart, 79(2)*:121-7, 1998.

Noor, E. T.; Das, R.; Lami, M. S.; Chakraborty, A. J.; Mitra, S.; Tallei, T. E.; Idroes, R.; Mohamed, A. A.-R.; Hossain, M. J.; Dhama, K.; Mostafa-Hedeab, G. & Emran, T. B. Ginkgo biloba: a treasure of functional phytochemicals with multimedicinal applications. *Evid. Based Complement. Alternat. Med., 2022*:8288818, 2022.

Ohkawa, H.; Ohishi, N. & Yagi, K. Assay for lipid peroxides in animal tissues by thiobarbituric acid reaction. *Anal. Biochem., 95(2)*:351-8, 1979.

Ono, K.; Iwasaki, Y.-K.; Akao, M.; Ikeda, T.; Ishii, K.; Inden, Y.; Kusano, K.; Kobayashi, Y.; Koretsune, Y.; Sasano, T.; *et al*. 2022 JCS/JHRS guidelines on pharmacotherapy of cardiac arrhythmias. *J. Arrhythm., 38(6)*:833-973, 2022.

Panday, S.; Talreja, R. & Kavdia, M. The role of glutathione and glutathione peroxidase in regulating cellular levels of reactive oxygen and nitrogen species. *Microvasc. Res., 131*:104010, 2020.

Pandita, D.; Pandita, A.; Wani, S. H.; Abdelmohsen, S. A. M.; Alyousef, H. A.; Abdelbacki, A. M. M.; Al-Yafrasi, M. A.; Al-Mana, F. A. & Elansary, H. O. Crosstalk of multi-omics platforms with plants of therapeutic importance. *Cells, 10(6)*:1296, 2021.

Popa, R.; Diaconu, M.; Cirlig, V.; Vaˇrut¸, C. M.; Caragea, D. C.; Codea, R. A.; Tabaran, F. A.; Aurori, M.; Gafencu, M. & Georgescu, C. C. Combination of pentoxifylline and *Ginkgo biloba* nephroprotective effect in animal models with vancomycin-induced nephrotoxicity. *Curr. Health Sci. J., 48(1)*:68-74, 2022.

Razná, K.; Sawinska, Z.; Ivanisová, E.; Vukovic, N.; Terentjeva, M.; Stricík, M.; Kowalczewski, P. L.; Hlavacková, L.; Rovná, K.; Ziarovská, J. & Kacániová, M. Properties of *Ginkgo biloba* L.: antioxidant characterization, antimicrobial activities, and genomic microRNA-based marker fingerprints. *Int. J. Mol. Sci.,21(9)*:3087, 2020.

Reeves, P. G.; Nielsen, F. H. & Fahey, G. C., Jr. AIN-93 purified diets for laboratory rodents: final report of the American Institute of Nutrition ad hoc writing committee on the reformulation of the AIN-76A rodent diet. *J. Nutr., 123(11)*:1939-51, 1993.

Rotruck, J. T.; Pope, A. L.; Ganther, H. E.; Swanson, A.; Hafeman, D. G. & Hoekstra, W. Selenium: biochemical role as a component of glutathione peroxidase. *Science, 179(4073)*:588-90, 1973.

Sagini, K.; Buratta, S.; Delo, F.; Pellegrino, R. M.; Giovagnoli, S.; Urbanelli, L. & Emiliani, C. Drug-induced lysosomal impairment is associated with the release of extracellular vesicles carrying autophagy markers. *Int. J. Mol. Sci., 22(23)*:12922, 2021.

Sakr, S. A. & El-Gamal, E. M. Effect of grapefruit juice on amiodarone-induced nephrotoxicity in albino rats. *Toxicol. Ind. Health, 32(1)*:68-75, 2016.

Samec, D.; Karalija, E.; Dahija, S. & Hassan, S. T. S. Biflavonoids: important contributions to the health benefits of Ginkgo (*Ginkgo biloba* L.). *Plants (Basel), 11(10)*:1381, 2022.

Santos, J. A.; Li, K. C.; Huang, L.; McLean, R.; Petersen, K.; Di Tanna, G. L. & Webster, J. Change in mean salt intake over time using 24-h urine versus overnight and spot urine samples: a systematic review and meta-analysis. *Nutr. J., 19(1)*:136, 2020.

Selamet, U.; Hanna, R. M.; Sisk, A.; Abdelnour, L.; Ghobry, L. & Kurtz, I. Rare onset of tubercular peritonitis amidst chronic renal dysfunction. *SAGE Open Med. Case Rep., 8*:2050313X20910029, 2020.

Shahidi, S.; Ghahremanitamadon, F.; Asl, S. S.; Komaki, A.; Afshar, S. & Hashemi-Firouzi, N. Electrophysiological, behavioral and molecular study of vitamin E and *Ginkgo biloba* in a rat model of Alzheimer's disease. *Res. J. Pharmacogn., 8*:39-51, 2021.

Shalen, E. F.; Heitner, S. B.; Al-Rashdan, L.; Akhavein, R.; Elman, M. R.; Fischer, K. L.; Lin, L. Q.; Mannello, M.; Nazer, B.; Song, H. K. & Masri, A. Perioperative amiodarone to prevent atrial fibrillation after septal myectomy in obstructive hypertrophic cardiomyopathy. *ESC Heart Fail., 8(6)*:4791-9, 2021.

Sinha, A. K. Colorimetric assay of catalase. *Anal. Biochem., 47(2)*:389-394, 1972.

Sndos, Z. & Al-Amri, S. M. Impact of *Ginkgo biloba* leaves extract on renal toxicity induced by amiodarone in male rats. *Int. J. Pharm. Phytopharmacol. Res. (eIJPPR), 9*:1-9, 2019.

Song, J.; Liu, D.; Feng, L.; Zhang, Z.; Jia, X. & Xiao, W. Protective effect of standardized extract of *Ginkgo biloba* against cisplatin-induced nephrotoxicity. *Evid. Based Complement. Alternat. Med., 2013*:846126, 2013.

Su, X.; Shi, R.; Hu, H.; Hu, L.; Wei, Q.; Guan, Y.; Chang, J. & Li, C. *Ginkgo biloba* extract attenuates renal injury induced by amiodarone in rats through antioxidant and anti-inflammatory mechanisms. *Molecules, 27(21)*:7479, 2022.

Tao, Y.; Zhu, F.; Pan, M.; Liu, Q. & Wang, P. Pharmacokinetic, metabolism, and metabolomic strategies provide deep insight into the underlying mechanism of *Ginkgo biloba* flavonoids in the treatment of cardiovascular disease. *Front. Nutr., 9*:857370, 2022.

Thind, M.; Zareba, W.; Atar, D.; Crijns, H.; Zhu, J.; Pak, H. N.; Reiffel, J.; Ludwigs, U.; Wieloch, M.; Stewart, J. & Kowey, P. Efficacy and safety of dronedarone versus placebo in patients with atrial fibrillation stratified according to renal function: post hoc analyses of the EURIDIS–ADONIS trials. *Clin. Cardiol., 45(1)*:101-9, 2022.

Torimitsu, T.; Yoshida, T.; Nishi, S.; Itoh, H. & Oya, M. Amiodarone-induced multiple organ damage in an Alström syndrome patient with end-stage renal disease and hepatic cirrhosis. *CEN Case Rep., 11*:11-6, 2022.

Tousson, E.; Atteya, Z.; El-Atrash, E. & Jeweely, O. I. Abrogation by *Ginkgo biloba* leaf extract on hepatic and renal toxicity induced by methotrexate in rats. *J. Cancer Res. Treat., 2*:44-51, 2014.

Tousson, E.; Keshta, A. T.; Hussein, Y.; Fekry, R. M. & Abo-Ghaneima, W. K. Renal protective effect of *Ginkgo biloba* and L-carnitine extracts against pentylenetetrazol-induced toxicity, oxidative stress, injury and proliferation alteration in epileptic rats. *Annu. Res. Rev. Biol., 32(2)*:1-13, 2019.

Tsukimura, T.; Shiga, T.; Saito, K.; Ogawa, Y.; Sakuraba, H. & Togawa, T. Differences in cleavage of globotriaosylceramide and its derivatives accumulated in organs of young Fabry mice following enzyme replacement therapy. *Mol. Genet. Metab. Rep., 28*:100773, 2021.

Tummino, T. A.; Rezelj, V. V.; Fischer, B.; Fischer, A.; O'Meara, M. J.; Monel, B.; Vallet, T.; Zhang, Z.; Alon, A.; O'Donnell, H. R.; *et al*. Phospholipidosis is a shared mechanism underlying the in vitro antiviral activity of many repurposed drugs against SARS-CoV-2. *bioRxiv, 2021*.03.23.436648, 2021.

Vamos, M.; Oldgren, J.; Nam, G. B.; Lip, G. Y. H.; Calkins, H.; Zhu, J.; Ueng, K. C.; Ludwigs, U.; Wieloch, M.; Stewart, J.; *et al*. Antithrombotic therapy in patients with atrial fibrillation undergoing percutaneous coronary intervention: an international consensus document. *Eur. Heart J. Cardiovasc. Pharmacother., 8(4)*:363-71, 2022.

Vasseur, M.; Jean, T.; Defeudis, F. V. & Drieu, K. *Ginkgo biloba* extract (EGb 761) and its protective effect against cerebral ischemia and reperfusion injury. *Gen. Pharmacol. Vasc. Syst., 25*:31-46, 1994.

Wang, H.; Chen, L.; Yang, B.; Du, J.; Chen, L.; Li, Y. & Guo, F. Protective effects of *Ginkgo biloba* extract against renal ischemia-reperfusion injury via antioxidant and anti-inflammatory mechanisms. *Nutrients, 15(8)*:1947, 2023.

Wang, J.; Qiu, X.; Xu, T.; Sheng, Z. & Yao, L. Protective effect of *Ginkgo biloba* extract against renal ischemia-reperfusion injury in rats. *Blood Purif., 47*:17-23, 2019.

Wang, K.; Ni, J.; Zhu, X.; Zhu, L.; Li, Y. & Zhou, F. *Ginkgo biloba* extract protects against renal ischemia-reperfusion injury by inhibiting oxidative stress and apoptosis. *Exp. Ther. Med., 22*:951, 2021.

Wang, Y.; Branicky, R.; Noë, A. & Hekimi, S. Superoxide dismutases: dual roles in controlling ROS damage and regulating ROS signaling. *J. Cell Biol., 217(6)*:1915-28, 2018.

Wei, C.; Zhang, Y.; Zhong, X.; Lu, S.; Zou, X.; Yang, Y.; Huang, S. & Huang, Z. *Ginkgo biloba* extract alleviates renal ischemia-reperfusion injury by modulating oxidative stress and inflammation. *Chin. Med., 17*:25, 2022.

Worth, H.; O'Hara, D. V.; Agarwal, N.; Collister, D.; Brennan, F. & Smyth, B. Symptom burden and health-related quality of life in patients with advanced chronic kidney disease who forgo dialysis. *Clin. J. Am. Soc. Nephrol., 17(6)*:911-21, 2022.

Zhu, W.; Barreto, E. F.; Li, J.; Lee, H. K. & Kashani, K. Drug-drug interaction and acute kidney injury development: a correlation-based network analysis. *PLoS One, 18(1)*:e0279928, 2023.

Corresponding author:
Prof. Dr. Refaat Ali Mohammed Eid
Department of Pathology
College of Medicine
King Khalid University
Abha
SAUDI ARABIA

E-mail: refaat_eid@yahoo.com